BRAIN CONNECTIVITY
Volume 3, Number 5, 2013

DOI: 10.1089/brain.2013.0171

Examination of Frontal and Parietal Tectocortical Attention Pathways in Spina Bifida Meningomyelocele Using Probabilistic Diffusion Tractography

Victoria J. Williams,[1] Jenifer Juranek,[2] Karla Stuebing,[3] Paul T. Cirino,[4] Maureen Dennis,[5] and Jack M. Fletcher[4]

Abstract

Abnormalities of the midbrain tectum are common but variable malformations in spina bifida meningomyelocele (SBM) and have been linked to neuropsychological deficits in attention orienting. The degree to which variations in tectum structure influence white matter (WM) connectivity to cortical regions is unknown. To assess the relationship of tectal structure and connectivity to frontal and parietal cortical regions, probabilistic diffusion tractography was performed on 106 individuals (80 SBM, 26 typically developing [TD]) to isolate anterior versus posterior tectocortical WM pathways. Results showed that those with SBM exhibited significantly reduced tectal volume, along with decreased fractional anisotropy (FA) in posterior but not anterior tectocortical WM pathways when compared with TD individuals. The group with SBM also showed greater within-subject discrepancies between frontal and parietal WM integrity compared with the TD group. Of those with SBM, qualitative classification of tectal beaking based on radiological review was associated with increased axial diffusivity across both anterior and posterior tectocortical pathways, relative to individuals with SBM and a normal appearing tectum. These results support previous volumetric findings of greater impairment to posterior versus anterior brain regions in SBM, and quantifiably relate tectal volume, tectocortical WM integrity, and tectal malformations in this population.

Key words: attention; diffusion tensor imaging; neural tube defect; spina bifida; superior colliculus; tectocortical pathways; white matter

Introduction

Spina bifida meningomyelocele (SBM), the most common congenital birth defect affecting the central nervous system worldwide, occurs in 0.3–0.5 per 1000 births annually in North America (Au et al., 2010). SBM is characterized as a neural tube defect leading to malformations of both spine and brain. Meningomyelocele is the most common and severe form of spina bifida, representing a protrusion of the spinal cord and meninges caused by incomplete fusion of the spine (Barkovich, 2005; Barkovich and Raybaud, 2012; Fletcher and Brei, 2010; Talamonti et al., 2007). The neuroanatomical abnormalities usually include atypical development and caudal herniation of the cerebellum and hindbrain (the Chiari II malformation) (Tubbs et al., 2004), which occurs in 90% of individuals with SBM (Barkovich, 2005; Barkovich and Raybaud, 2012; Juranek et al., 2010; Juranek and Salman, 2010). The aberrant configuration of the hindbrain resulting from the Chiari II malformation obstructs the flow of cerebrospinal fluid at the level of the fourth ventricle, leading to hydrocephalus in 80–90% of children with SBM, 50–80% of whom require the insertion of a shunt (Bowman and McLone, 2010; Reigel and Rotenstein, 1994).

The Chiari II malformation is associated with a spectrum of abnormalities that appear variably in SBM, including kinking of the medulla, and midbrain anomalies, such as beaking of the tectum (Juranek and Salman, 2010; Tubbs et al., 2004). The consequences of tectal beaking (Fig. 1), frequently visualized in imaging studies of individuals with SBM, are unclear; for example, it is not known whether the aberrant structural

[1]Department of Psychology, University of Houston, Houston, Texas.
[2]Department of Pediatrics, University of Texas Health Science Center, Houston, Texas.
[3]Texas Institute for Measurement, Evaluation, and Statistics (TIMES), University of Houston, Houston, Texas.
[4]Department of Psychology, Texas Institute for Measurement, Evaluation, and Statistics (TIMES), University of Houston, Houston, Texas.
[5]Department of Surgery and Psychology, University of Toronto, Toronto, Canada.

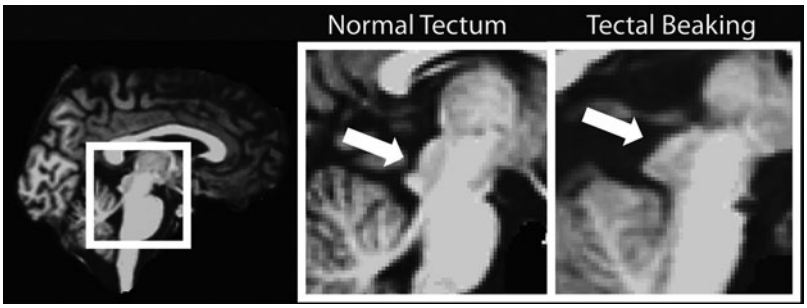

FIG. 1. Depiction of a normal appearing tectum in an individual with SBM (left) versus an individual with SBM demonstrating tectal beaking (right). SBM, spina bifida meningomyelocele.

formation of the tectum contributes to compromised or altered connectivity of white matter (WM) between this region and its cortical projections. Regardless, there are consistent findings linking qualitative abnormalities of the tectum to deficits in attention orienting in SBM (Dennis et al., 2005a).

Attention orienting in SBM

Functionally, the tectum is considered critical to spatial attention as a component of the posterior attention network subserving attention orienting and shifting (Posner and Petersen, 1990). Earlier research has demonstrated specific deficits in attention orienting in children with SBM, with tectal beaking associated with a greater degree of attentional impairment. In particular, children with SBM and tectal beaking show deficits in covert orienting, as well as a higher cost of disengagement from currently selected stimuli when compared with controls, and with children with SBM and no tectal dysmorphometry (Dennis et al., 2005a). Children with SBM also demonstrate attenuated inability to re-engage a new target on a task measuring inhibition of return, with greater decrements in performance among children exhibiting tectal beaking (Dennis et al., 2005b). These types of attention problems can be observed even in infancy, because basic orienting ability is impaired in infants with SBM (Taylor et al., 2010). Despite the evidence for tectal dysmorphometry contributing to decrements in attentional ability in SBM, there have been no quantitative analyses of tectal dysmorphmetry and the integrity of efferent pathways subserving attentional processing in SBM, which involve tectal structures.

Anatomy and function of the tectum

The tectum (comprising both inferior and superior colliculi) is the only midbrain structure that resembles the laminar organization and hierarchical processing evidenced in higher-order cortex (Merker, 2007). The superior colliculi are topographically organized to contain layered spatial maps from various sensory modalities, which overlap and correspond to one another via spatial coordinates. Anatomically, the superior colliculus (SC) is divided into a superior and intermediate division, differentiated by neuronal structure and function. The superficial layer of the SC only receives direct, one-way input from primary sensory regions, including the retina, visual cortex, and extrastriate pathways (Knudsen, 2011), with outputs projecting to visuomotor and motor neurons located immediately inferior within the intermediate layer of the SC. The intermediate layer has been determined a critical site for the convergence and integration of primary sensory inputs with other higher-order projections from visual and nonvisual cortical regions involved in spatial attention, including the parietal, prefrontal, and temporal regions (Merker, 2007).

Modulating spatial attention is an important function of the human brain and subserves attending to salient cues in the environment, along with the selection of relevant stimuli as the focus for subsequent cognitive processing. The midbrain SC, in conjunction with fronto-parietal cortical networks, supports attention orienting (Knudsen, 2011). Although the SC is classically considered important for the generation of saccadic eye movements during both voluntary and reflexive visual orienting, primate studies have identified the importance of the SC in covert shifts of attention without a motor response(Ignashchenkova et al., 2004), as well as a critical role in attentional selection (Lovejoy and Krauzlis, 2010) and perceptual bias of visual stimuli (Nummela and Krauzlis, 2010).

In humans, isolated lesions to the SC are rare, although a case study of a patient with thiamine deficiency accompanied by a collicular lesion showed a complete absence of inhibition of return on a covert spatial orienting task (Sereno et al., 2006). A study utilizing functional magnetic resonance imaging (fMRI) revealed significant activation of the SC in an exploratory attention paradigm, identifying functional connectivity between the SC and the right frontal eye field, and bilateral parietal and occipital cortices (Gitelman et al., 2002). Thus, evidence from both human and primate studies indicates that the SC is involved in the process of target selection for both overt orienting eye movements (shift of gaze to orient toward salient visual stimuli) and the allocation of covert spatial attention (a shift of visuo-spatial attention without eye movements) (Knudsen, 2011; Mysore and Knudsen, 2011).

Rationale for the present study

In SBM, congenital hydrocephalus primarily disrupts WM in posterior regions (Simpson et al., 2011), potentially impacting functional connectivity between parietal visuo-spatial processing regions and the midbrain tectum, modulating attentional selection. In addition, congenital tectal malformations and decreased cortical gray matter in the posterior lobes of children with SBM (Juranek and Salman, 2010) may also contribute to previously observed difficulties with attention orienting. Thus, SBM permits investigation into potential dissociations of underlying WM connectivity subserving theoretically proposed anterior versus posterior tectocortical pathways of attention orienting, while also providing a quantitative structural examination of the midbrain tectum.

Table 1. Demographic Information

	TD (n = *26*)	*SBM-NT* (n = *29*)	*SBM-TB* (n = *51*)
Years of age at MRI (M[SD])	13.89 (5.70)	15.11 (5.78)	13.40 (4.00)
SES (M[SD])[+,*]	41.02 (10.36)	31.90 (14.14)	34.03 (12.68)
Gender (% Male)	62	48	57
Ethnicity (% of group)			
Hispanic	58	59	53
Non-Hispanic	42	41	47
African American	11	3	14
Asian	8	0	0
Caucasian	19	38	31
Other	4	0	2
IQ (M[SD])*	102.92 (10.23)	88.34 (14.84)	80.25 (13.25)

[+]One SBM participant missing data for SES.
*$p < 0.01$.
M, mean; SD, standard deviation; SBM, spina bifida meningomyelocele; NT, normal appearing tectum; TB, tectal beaking; TD, typically developing; SES, socio-economic status; IQ, Stanford Binet Composite score; MRI, magnetic resonance imaging.

The current study examined the structural integrity of WM tectocortical pathways between the colliculus and frontal/parietal cortical regions implicated in attention orienting using diffusion tensor imaging (DTI) probabilistic tractography procedures, as well as volumetric analysis of the tectum in children with SBM. We hypothesized:

1. Because individuals with SBM show volumetric reductions in WM primarily in posterior as opposed to anterior brain regions, we predicted that individuals with SBM (both with and without tectal beaking) would have reduced indices of WM integrity along parietal but not frontal tectocortical pathways compared with typically developing (TD) individuals. In addition, we predicted that those with tectal abnormalities would have reduced WM integrity within both frontal and parietal tectocortical pathways compared with individuals with SBM and a normal appearing tectum.
2. Mean DTI metrics of frontal versus parietal tectocortical pathways are difficult to meaningfully compare within participants, because raw values may be confounded by differing degrees of tract length and variations in extent of crossing fibers along each tract. Therefore, a ratio was calculated for each participant dividing frontal by parietal DTI metrics as a within-subject indicator of discrepancy between frontal and parietal tract integrity. We predicted greater discrepancy between frontal and parietal WM indices in individuals with SBM relative to controls.
3. We predicted a significant reduction in overall tectal volume between SBM individuals with qualitative tectal beaking compared with SBM cases with a normal appearing tectum and TD controls.

Methods

Participants

The sample consisted of 80 individuals with SBM and 26 TD comparisons. The volunteers in the comparison group were selected in the same age range (8–29 years) as the group with SBM, and had no history or evidence of neurologic or neurodevelopmental disorders. Participants with SBM were recruited through clinics and parent advocacy groups for SBM.

All of the participants with SBM were medically stable and had IQ scores above the level associated with intellectual disabilities (standard scores > 70). Of the 80 individuals with SBM, 29 showed a normal appearing tectum (SBM-NT), while 51 exhibited tectal beaking based on radiological review (SBM-TB). Table 1 shows that the groups with SBM and the TD group did not differ in age, $F(2,103) = 1.12$, $p = 0.33$; sex, $\chi^2(2) = 1.04$, $p = 0.60$; or Hispanic versus non-Hispanic ethnicity, $\chi^2(2) = 0.299$, $p = 0.86$. Sex or ethnicity did not explain a significant amount of outcome variance in any of the models and were not included as covariates. Consistent with earlier studies (Fletcher et al., 2005), the groups differed on a measure of socioeconomic status (SES), $F(2,102) = 4.0$, $p = 0.02$, with TD individuals having a significantly higher SES than both the SBM group with a normal appearing tectum $t(53) = 2.65$, $p = 0.01$, and the SBM group exhibiting tectal beaking $t(74) = 2.30$, $p = 0.02$; the two SBM groups did not differ from one another. However, SES was not significantly correlated with any of the outcome variables as well.

Table 2 shows that the majority of those with SBM were radiologically coded with a Chiari II malformation of the hindbrain accompanied by a hypoplastic or dysgenetic corpus callosum. Exceptions included three participants with a Chiari I malformation, and seven participants with no observed Chiari malformation of either type. Of those seven with no Chiari, aqueductal stenosis accounted for hydrocephalus in six participants. Overall, the sample of individuals with SBM and hydrocephalus is representative of the overall population with the majority evidencing predominantly lower spinal lesions, ambulatory difficulties, no seizure history, and two to four shunt revisions (Fletcher et al., 2005). The number of shunt revisions did not significantly account for variance in outcome variables in any of the models and was not utilized as a covariate.

MRI data acquisition

T1-weighted acquisition. A three-dimensional, whole-brain high-resolution, T1-weighted scan was collected for each participant in the coronal plane using Sensitivity Encoding (SENSE) technology. Scans were acquired using a Philips 3.0 T Intera system with the following parameters: repitition time (TR)/echo time (TE) = 6.5–6.7/3.04–3.14 msec; flip angle = 8°;

Table 2. SBM Characteristics

	% of SBM-NT (n = 29)	% of SBM-TB (n = 51)
Lesion level		
Above L1	0	28
Below T12	100	72
Chiari malformation		
None	21	2
Type I	10	0
Type II	69	98
Corpus collosum		
Normal	7	2
Hypoplastic	72	60
Dysgenetic	21	38
Shunt revisions		
Unknown	0	2
None	21	14
1	21	31
2–4	51	43
5–9	7	8
>10	0	2
Ambulatory status		
Normal	14	0
Independent	24	26
With support	41	31
Unable	21	43
Seizure disorder		
No	84	90
Past	3	8
Present	3	2

square field of view (FOV) = 24 cm^3; matrix = 256 × 256; slice thickness = 1.5 mm; in-plane pixel dimensions (x,y) = 0.94, 0.94; and number of excitations (NEX) = 2.

DTI acquisition. DTI image acquisition employed a single-shot spin-echo diffusion sensitized echo-planar imaging sequence with the balanced *Icosa21* encoding scheme, which uses 21 uniformly distributed diffusion encoding orientations, with the following DTI parameters: TR = 6100 msec; TE = 84 msec; 44 slices total; square FOV = 24 cm^3; acquisition matrix = 256 × 256; slice thickness = 3 mm; and b value = 1000 sec/mm^2. A single nondiffusion weighted or "low b" image with a b value = 0 sec/mm^2 was acquired as an anatomical reference volume. In addition, each encoding was repeated twice and magnitude-averaged to enhance the signal-to-noise ratio. The total DTI acquisition time was ~7 min, with the entire MRI exam less than 30 min to accommodate pediatric participants.

MRI and DTI processing

T1-weighted imaging analysis. T1-weighted images were processed using the FreeSurfer image analysis suite (http://surfer.nmr.mgh.harvard.edu/) for the labeling of cortical regions of interest used as tractography endpoint masks (Dale et al., 1999; Fischl et al., 1999, 2001, 2002, 2004a, 2004b). The T1-weighted image and corresponding cortical segmentation labels were nonlinearly co-registered and transformed into native DTI space to serve as anatomical endpoints for tractography procedures, and then slightly dilated to extend 2 mm deeper into directly adjacent WM to aid in fiber tracking.

DTI preprocessing procedures. DTI data processing utilized diffusion tools available as a part of the FreeSurfer and FSL (www.fmrib.ox.ac.uk.ezp-prod1.hul.harvard.edu/fsl) processing streams. Diffusion volumes underwent eddy current and motion correction. The diffusion tensor was then calculated for each voxel using a least-squares fit to the log of the diffusion signal. The T2-weighted lowb volume was skull stripped (Smith, 2002), and served as a brain mask for all other diffusion maps. Maps for fractional anisotropy (FA), axial diffusivity [λ_1] (AD), and radial diffusivity [$(\lambda_2 + \lambda_3)/2$] (RD) were then isolated for further FSL tractography processing and analysis.

Labeling of collicular seed region. Hand-drawn regions of interest (ROI) defining the complete left and right divisions of the midbrain tectum were created for each subject (by a single rater blinded to diagnosis), to serve as seed regions in subsequent probabilistic tractography procedures and to determine tectal volume. Although the SC is the primary structure of interest, the label included the entire tectum (both superior and inferior colliculi) to accommodate individuals with SBM who exhibited tectal beaking where both inferior and superior sets of colliculi merge to form an indistinguishable "beak" of tissue (Fig. 1). Hand-drawn ROIs were created using a mouse to label voxels in fslview within the axial acquisition plane of the T2-weighted lowb image acquired as an anatomical reference volume within the DTI sequence. The number of axial slices to demarcate the tectum ranged from 3–5, with a slice thickness of 3 mm. By directly labeling the T2-weighted lowb image acquired in each subject's native DTI space, the resultant label directly corresponded to the intended collicular tractography seed point, requiring no transformations reliant on co-registration procedures. Due to common structural brain abnormalities in children with SBM, nonlinear co-registration techniques appeared less robust than would be expected with a typical adult brain, and minimizing the need for registration-based transformations was considered advantageous in the labeling of subcortical midbrain structures in this population. Intra-rater reliability was assessed using the Dice similarity coefficient (DSC), which is a variation of the kappa statistic commonly used in reliability analysis. The DSC procedure assesses not only the reliability of the number of voxels between tracings, but also the spatial overlap of retraced voxels. The mean intra-rater DSC calculated using a randomly selected 10% of cases was 0.894 (range, 0.850–0.927), where values of DSC above 0.7 are usually considered a satisfactory level of agreement between two segmentations (Entis et al., 2012; Xue et al., 2007; Zijdenbos et al., 1994).

Diffusion tensor seed-based probabilistic tractography. In preparation for tractography procedures, four-dimensional data, including both diffusion-weighted and lowb volumes, were fed into FSL's bedpostx tool to calculate the Bayesian estimate of diffusion parameters obtained using sampling techniques. Monte–Carlo sampling accumulated distributions of diffusion parameters at each voxel (allowing for multiple fiber orientations per voxel) and created necessary files to run probabilistic tractography. Probabilistic tractography was subsequently performed using probtracx, as a part of the FMRIB's Diffusion Toolbox (Behrens et al., 2003).

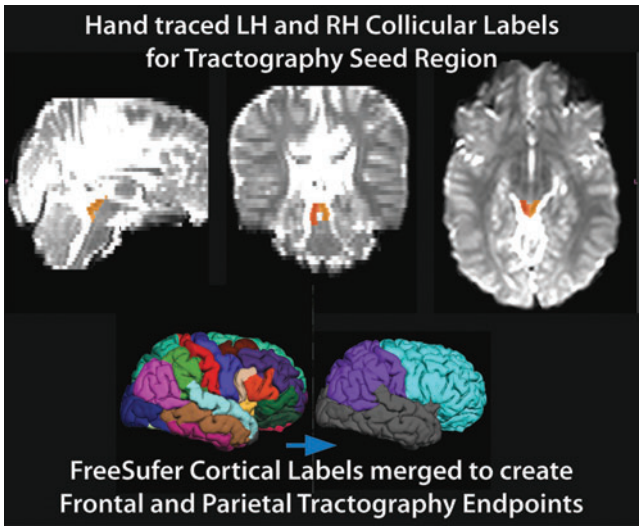

FIG. 2. Example of manually traced collicular seed point labels (right = orange, left = yellow) on lowb DTI image, and merging of FreeSurfer's automated cortical parcellation labels to achieve frontal (turquoise) and parietal (purple) cortical endpoint masks. DTI, diffusion tensor imaging; LH, left hemisphere; RH, right hemisphere.

The seed point for these connectivity distributions was generated from hand-drawn labels of the midbrain tectum as defined earlier. An endpoint was also specified to limit tractography procedures only to defined WM pathways terminating within these cortical labels. Visualization of manually traced collicular seed labels and FreeSurfer-derived automated cortical labels are presented in Figure 2. Probabilistic tractography was conducted for each hemisphere independently using either left or right collicular seed points. For each hemispheric seed point, two probabilistic tractography iterations were performed defining WM connectivity from the colliculi to parietal or frontal cortical regions independently.

Since tectal volume varies between individuals, and as the number of tractography iterations performed was a function of the number of voxels within the seed region (5000 iterations per voxel), a normalization postprocessing procedure was implemented to standardize final tract output across participants. This was accomplished by dividing the probability density function for each voxel by the total number of successful iterations performed within subject (waytotal), resulting in a normalized value that could be interpreted as the tract probability given the prior knowledge that the tract exists on that voxel. Normalization procedures aimed at control for volumetric differences in seed regions between participants, in addition to providing a common-scale indicator of tract strength, allowing for proportional thresholding across all individuals to isolate regions with the most robust connectivity. After normalization of tracts, a standardized threshold was determined by excluding voxel intensities below the 95th percentile value of the normalized distributions, averaged across all participants and pathways (mean = 0.01, SD = 0.02). Results of thresholding at the average 95th percentile yielded robust pathways of interest for all participants while excluding extraneous pathways. Subsequent to waytotal normalization, resulting maps were further thresholded to remove voxels in which the FA value is less than 0.2 to limit inclusion of non-WM tissue such as ventricles, shunt pathways, and cortex. Similar normalization and thresholding procedures have been implemented in earlier studies utilizing FSL probabilistic tractography procedures (Caspers et al., 2011; Li et al., 2010). Finally, thresholded output was then

Table 3. Means and Standard Deviations of Dependent Variables

	SBM					
	Tectal beaking (n = *51*)		*Normal tectum* (n = *29*)		*TD* (n = *26*)	
	M	*SD*	*M*	*SD*	*M*	*SD*
Fractional anisotropy ($\times 10^{-6}$ mm^2/sec)						
Frontal	0.4416[a]	0.0349	0.4365[a]	0.0429	0.4431[a]	0.0178
Parietal	0.4310[a]	0.0295	0.4326[a]	0.0365	0.4543[b]	0.0168
Radial diffusivity ($\times 10^{-3}$ mm^2/sec)$^+$						
Frontal	598.3[a]	43.6	584.8[a]	48.7	562.2[b]	21.7
Parietal	641.3[a]	57.6	614.8[a]	49.5	571.5[b]	21.6
Axial diffusivity ($\times 10^{-3}$ mm^2/sec)$^+$						
Frontal	1227.7[a]	57.4	1189.1[b]	30.1	1165.2[b]	20.8
Parietal	1284.0[a]	75.4	1238.7[b]	34.6	1212.6[b]	22.3
Tectal volume (mm^3)						
Right tectal volume	773.8[a]	204.7	781.7[a]	199.9	993.8[b]	286.2
Left tectal volume	793.4[a]	202.4	790.4[a]	213.1	1022.0[b]	316.8
Total tectal volume	1567.3[a]	394.7	1572.0[a]	398.7	2015.9[b]	587.7
Pathway volume (mm^3)						
Frontal pathway	12297[a]	2772	12513[a]	2327	12921[a]	1131
Parietal pathway	10624[a]	2241	10941[a]	2307	11176[a]	1135

[+]Value multiplied by factor of 1000; differences in alphabetic superscript for means denotes significant analysis of covariance between groups at $p < 0.01$, means with the same superscript do not significantly differ; diffusion tensor imaging metrics include age as covariate, volumetric measurements include brain volume excluding CSF as covariate.

CSF, cerebrospinal fluid.

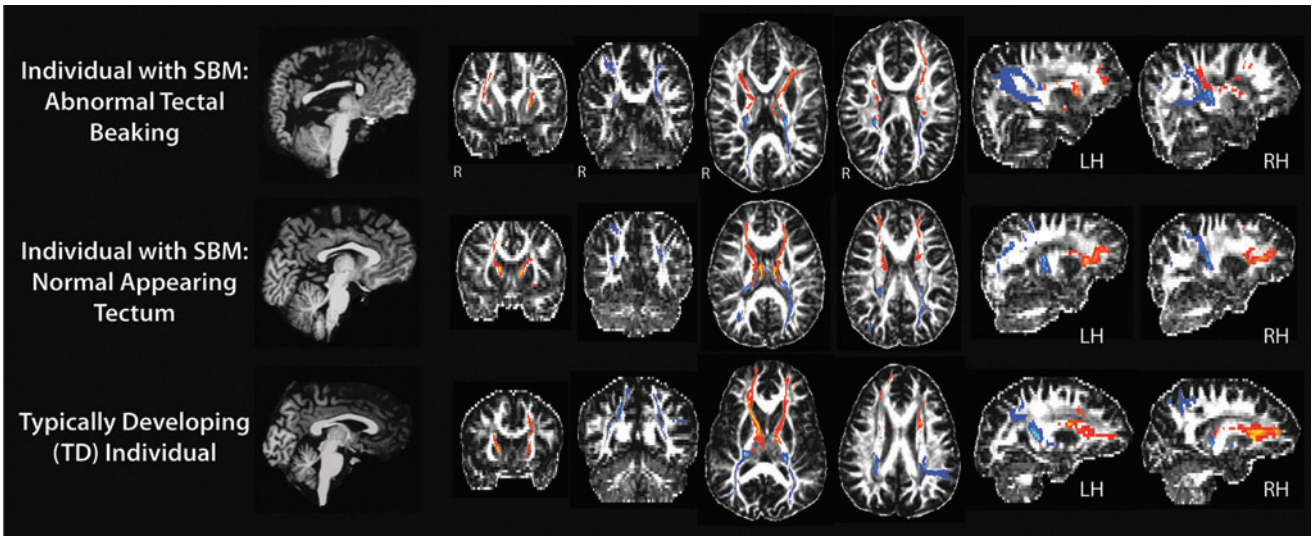

FIG. 3. Sample of probabilistic tractography results of frontal (red) and parietal (blue) tectocortical pathways in TD and SBM individuals with and without tectal abnormalities. TD, typically developing.

binarized and served as tractography-derived masks to extract the mean fractional anisoptopy, RD, and AD for each participant.

Results

Output of probabilistic diffusion tractography

Average diffusivity metrics were calculated for each participant based on the output of seed-based probabilistic tractography procedures modeling tectocortical connectivity for each hemisphere. No group showed significant hemispheric differences with regard to indicators of WM tract integrity, so left and right hemisphere measurements were averaged within participants to provide a single indicator depicting frontal versus parietal tract characteristics. Mean values of FA, RD, and AD for each pathway for the groups with SBM (with and without tectal beaking) and the TD group are presented in Table 3. Analysis of variance (ANOVA) indicated that groups did not significantly differ in the number of voxels resulting from probabilistic tractography procedures defining frontal [$F(2,103) < 1$] or parietal [$F(2,103) < 1$] tectocortical pathways.

Output of resultant tectocortical pathways from a representative participant within each group is presented in Figure 3. A qualitative examination of resulting pathways across both TD and SBM individuals revealed bilateral projections emanating from the colliculus to cortical endpoints. Tractography constrained to frontal lobe endpoints showed fiber pathways ascending through the thalamus, anterior continuation along the internal capsule, with the majority of fibers terminating in WM subjacent to precentral, rostral middle frontal, and superior frontal cortex. Parietal pathways also

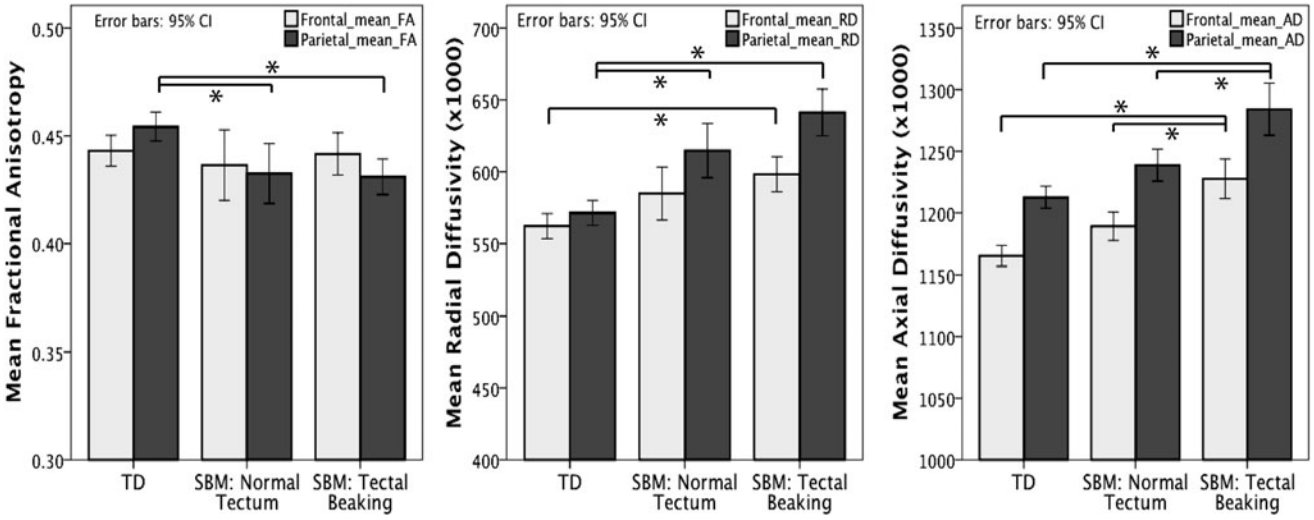

FIG. 4. Mean values of FA, RD, and AD showing a 95% confidence interval between TD and SBM individuals grouped by tectal beaking along frontal (gray) and parietal (black) tectocortical pathways. *$p < 0.01$. AD, axial diffusivity; FA, fractional anisotropy; RD, radial diffusivity.

traversed anteriorly through the thalamus, with projections that quickly ascended along medial tracts of the posterior thalamic radiation following the lateral ventricles, and terminating in WM subjacent to the cortex within postcentral, inferior, and superior parietal regions.

Hypothesis 1: frontal and parietal tectocortical pathways

Group means and standard deviations of FA, RD, and AD along frontal and parietal pathways are presented in Table 3. Analysis of covariance (ANCOVA) was conducted between TD participants and individuals with SBM subdivided into those with a normal appearing tectum, and those exhibiting qualitative tectal beaking, with age as a covariate. The family-wise error rate for the first hypothesis was controlled using the Bonferonni approach (0.5/6, critical alpha = 0.008), with follow-up pairwise comparisons maintained at a critical alpha of 0.05 based on Fisher's Least-Significance Difference test with three groups (Maxwell and Delaney, 2004). Mean values of DTI metrics fitted with a 95% confidence interval for each group are presented as a bar graph in Figure 4.

Fractional anisotropy. Variance of mean FA along frontal pathways was not significantly accounted for by age and group, and the overall model did not reach the critical level of alpha, Adj. $R^2 = 0.021$; $F(3,102) = 1.759$, $p = 0.160$.

Results of ANCOVA indicated a significant overall model fit, as group and age accounted for 12.5% of variance along parietal tectocortical pathways [Adj. $R^2 = 0.125$; $F(3,102) = 6.0$, $p = 0.001$], with a significant main effect of group [$F(2,102) = 6.23$, $p = 0.003$]. *Post-hoc* pairwise analyses revealed significantly higher mean FA along parietal tracts among TD individuals compared with those with SBM both with a normal appearing tectum, [$t(52) = 3.01$, $p = 0.01$] and those with tectal beaking [$t(74) = 3.27$, $p = 0.004$]. There were no differences in parietal FA between the two SBM groups.

Radial diffusivity. Along frontal tectocortical pathways, 16% of the variance in mean RD could be attributed to the overall model specifying group and age [Adj. $R^2 = 0.16$; $F(3,102) = 7.65$, $p < 0.001$], with the group showing a significant main effect [$F(2,102) = 6.75$, $p = 0.002$]. Pairwise comparisons (Fig. 4) indicated significantly higher mean RD along frontal tracts in individuals with SBM evidencing tectal beaking compared with TD participants [$t(74) = 3.66$, $p = 0.001$]. Individuals with SBM classified by a normal appearing tectum did not significantly differ in mean RD along frontal pathways from those with tectal beaking [$t(77) = 1.02$, $p = 0.94$], or TD participants [$t(52) = 2.38$, $p = 0.06$].

The overall model explained a significant amount of the variance in RD (29.3%) along parietal tectocortical tracts [Adj. $R^2 = 0.293$; $F(3,102) = 7.65$, $p < 0.001$]. The main effect of the group was statistically significant [$F(2,102) = 15.48$, $p < 0.001$]. Follow-up analyses indicated significantly lower mean RD in TD individuals compared with those with SBM classified with a normal appearing tectum [$t(52) = 3.65$, $p = 0.001$], or tectal beaking [$t(74) = 6.014$, $p < 0.001$]. Of those with SBM, mean RD in parietal pathways did not significantly differ when classified by normal or atypical tectal formation [$t(77) = 1.96$, $p = 0.16$].

Axial diffusivity. In frontal pathways, 26.9% of the variance in mean AD could be accounted for by the overall model [Adj. $R^2 = 0.269$; $F(3,102) = 13.91$, $p < 0.001$], with a significant group effect [$F(2,102) = 18.28$, $p < 0.001$]. Pairwise comparisons (Fig. 4) revealed no significant difference in mean frontal AD between TD participants and those with SBM with a normal appearing tectum [$t(52) = 2.17$, $p = 0.10$]. Individuals with tectal beaking evidenced significantly higher mean AD than both the TD group [$t(74) = 5.85$, $p < 0.001$] and those with SBM showing a normal appearing tectum [$t(77) = 3.50$, $p = 002$].

Along parietal pathways, 23.4% of the variance in mean AD could be explained by the overall model [Adj. $R^2 = 0.234$; $F(3,102) = 11.68$, $p < 0.001$], with a significant group effect [$F(2,102) = 14.670$, $p < 0.001$]. Pairwise comparisons along parietal pathways revealed no significant difference in mean AD between the TD and the SBM group with a normal appearing tectum [$t(52) = 1.90$, $p = 0.18$]. Those with tectal beaking revealed significantly higher mean AD when compared with both TD participants [$t(74) = 5.23$, $p < 0.001$] and those with SBM evidencing a normal appearing tectum [$t(77) = 3.17$, $p = 0.006$].

Hypothesis 2: within-subject ratios of mean frontal by mean parietal diffusivity metrics

To assess the degree of discrepancy between frontal and parietal tectocortical WM integrity within individuals, a ratio relating mean frontal to mean parietal diffusivity measures was calculated for each participant per DTI metric (FA, AD, and RD):

$$\text{Ratio} = \frac{\text{Mean Frontal DTI Metric}}{\text{Mean Parietal DTI Metric}}$$

The means of the calculated ratios fitted with a 95% confidence interval for each group are presented as a bar graph in Figure 5. A ratio value of 1 represents no within-subject difference in DTI metrics between pathways, where ratios >1 represent higher values in frontal compared with parietal and <1 indicates higher DTI metrics in parietal compared with frontal tracts. To compare within-subject ratios between

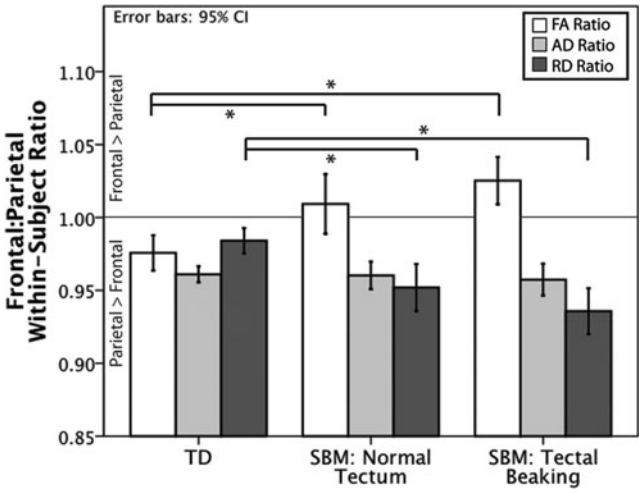

FIG. 5. Mean frontal:parietal ratio for DTI metrics (FA, RD, and AD) by group, with error bars representing a 95% confidence interval. TD individuals had significantly less discrepancy between frontal and parietal mean RD and frontal FA compared with those with SBM (regardless of the presence of tectal abnormalities). Groups did not significantly differ among AD ratios. *$p < 0.01$.

the three groups, a one-way ANOVA was conducted, with family-wise error controlled using the Bonferonni approach (0.5/3, critical alpha = 0.016). Significant main effects of group were followed up with *post-hoc* pairwise comparisons, correcting for multiple comparisons using the Least-Significant Difference test with three groups, maintaining a critical alpha of 0.05 (Maxwell and Delaney, 2004). Since the dependent variable (frontal/parietal ratio) is a within-subject comparison, age was not included in the model as a covariate.

FA ratio. Ratios relating frontal to parietal mean FA within subjects significantly differed by group [Adj. $R^2 = 0.120$; $F(2,103) = 7.65$, $p < 0.001$]. Follow-up pairwise comparisons indicated that individuals with SBM either with [$t(75) = 2.43$, $p = 0.05$] or without tectal beaking [$t(53) = 4.17$, $p < 0.001$] had a significantly greater ratio that was indicative of higher FA in frontal compared with parietal tracts than TD individuals, who showed the opposite pattern with a ratio less than 1. There were no significant differences in FA ratios between the two SBM groups [$t(78) = 1.33$, $p = 0.54$].

RD ratio. A between-group comparison of ratios relating within-subject frontal to parietal mean RD indicated a significant group effect [Adj. $R^2 = 0.139$; $F(2,103) = 9.483$, $p < 0.001$]. Follow-up pairwise comparisons revealed smaller ratios relating frontal to parietal mean RD values for individuals with SBM exhibiting tectal beaking [$t(75) = 4.34$, $p < 0.001$], and those with SBM showing a normal appearing tectum [$t(53) = 2.67$, $p = 0.03$], compared with TD participants. There was no significant difference in RD frontal:parietal discrepancy between the two SBM groups [$t(78) = 1.46$, $p = 0.40$].

AD ratio. A between-group comparison of ratios relating frontal to parietal mean AD within subjects revealed no significant differences between TD participants, and those with SBM with or without tectal beaking [Adj. $R^2 = 0.016$; $F(2,103) = 0.156$, $p = 0.856$].

Hypothesis 3: tectal volume

To assess differences in tectal volume, total brain volume excluding cerebrospinal fluid (CSF) was included as a covariate to control for variations in tectal volumetric measurements related to cranial size. Total brain volume (as opposed to intracranial volume) was determined as the best common denominator for scaling in both cohorts to avoid biasing due to enlarged ventricles/craniums among individuals with SBM. In the overall model, group and total brain volume without ventricles accounted for 14.9% of the variance in total tectal volume [Adj. $R^2 = 0.15$; $F(3,102) = 7.13$, $p < 0.001$]. Results indicated a significant effect of group [$F(2,102) = 6.61$, $p = 0.002$]. Follow-up pairwise comparisons revealed a significantly larger tectal volume in TD individuals compared with individuals with SBM, both those exhibiting tectal beaking [$t(74) = 3.51$, $p < 0.001$], and those with a normal appearing tectum [$t(52) = 2.97$, $p = 0.004$]. There was no significant group difference in tectal volume between individuals with SBM with and without tectal beaking [$t(77) < 1$].

Discussion

Tectal beaking is poorly understood, with descriptions largely clinical and no existing volumetric or connectivity analyses. In this study, there were significant associations between variations in both qualitative and quantitative properties of the midbrain tectum in SBM, and connectivity of this structure to cortical networks subserving attention processes. These results have two major implications. First, there is greater disruption of posterior brain morphology in those with SBM compared with TD individuals, which is consistent with earlier research. Second, tectal beaking in SBM was associated with decreased indices of WM integrity across both frontal and parietal tectocortical pathways compared not only with TD controls, but also with individuals with SBM and a normal appearing tectum. Tectal beaking was associated with increased AD, in which individuals with SBM and a normal appearing tectum did not significantly differ from the TD comparison group. Thus, changes in AD along all pathways emanating from the colliculus may be uniquely related to developmental malformation of this structure in SBM and not simply to the mechanical effects of hydrocephalus, thus providing a potential mechanism for spatial attention deficits in SBM (Dennis et al., 2005a, 2005b).

Discrepancy in frontal and parietal WM in SBM

In support of the first hypothesis, individuals with SBM (regardless of tectal beaking) exhibited significantly decreased mean FA and increased mean RD along parietal tectocortical pathways, with fewer differences along frontal tracts (Fig. 4). Although earlier studies have demonstrated opposing findings of decreased FA in isolated frontal regions of interest within the genu of the corpus callosum, fornix, and cingulum in those with SBM (Herweh et al., 2009; Vachha et al., 2006), congenital malformations such as callosal hypogenesis along with the vulnerability of periventricular WM to structural insult after hydrocephalus may explain such decrements. Comparable FA along frontal WM pathways among the groups with SBM and TD individuals is supported by the preservation of anterior structural features in regions spared from the periventricular insults of hydrocephalus, such as preserved cortical thickness within the frontal lobes in SBM (Juranek et al., 2008). Thus, results were congruent with earlier studies indicating preferential insult to posterior pathways in SBM while adding the new information that anterior WM is relatively intact.

Consistent with the second hypothesis, individuals with SBM significantly differed on within-subject frontal:parietal tectocortical tract ratios than TD participants (Fig. 5). Individuals with SBM, regardless of the presence of tectal beaking, exhibited decreased FA and increased RD along parietal tracts relative to frontal tectocortical pathways. Thus, significant group differences observed in diffusivity metrics along individual tracts may also be interpreted based on within-subject discrepancies between frontal and parietal WM integrity.

In animal models, observed alterations in posterior WM morphology have been largely attributed to the mechanical effects of hydrocephalus because of the accumulation of cerebral spinal fluid in the lateral ventricles, which exerts pressure and expands tissue along a posterior to anterior gradient. Periventricular WM, especially long pathways extending between the brainstem and cortical regions much similar to the parietal tectocortical tract observed in the present study, are distinctly vulnerable to the effects of hydrocephalus.

Hydrocephalus alters myelin integrity in hydrocephalic rat models through a loss of oligodendrocytes (Olopade et al., 2012), which is congruent with findings of the current study revealing increased RD as a possible indicator of altered myelin integrity among individuals with SBM (Budde et al., 2007; Concha et al., 2006; Song et al., 2003).

A similar pattern of decreased FA and increased RD was previously observed in a DTI study examining children with hydrocephalus (Yuan et al., 2013). Earlier human imaging and autopsy studies have also related a disruption of myelination processes consequential to the occurrence of hydrocephalus and associated increases in intracranial pressure (Gadsdon et al., 1979; Hanlo et al., 1997). The endurance of neuronal changes after acute intervention for ventriculomegaly has been addressed within hydrocephalic animal models investigating the potential restoration of impaired axonal connectivity to cortical regions. These studies revealed some evidence of improvement, but not complete recovery of axons after ventricular shunting procedures (Aoyama et al., 2006; Eskandari et al., 2004).

Changes in WM integrity unique to tectal beaking in SBM

Another salient finding was that mean AD was uniquely associated with the presence of tectal malformation. Individuals with SBM and tectal beaking had higher mean AD along both frontal and parietal pathways when compared with SBM individuals with a normal tectum and with TD controls; the latter two groups with normal tecti were not distinguishable in measures of AD (Fig. 4). Interestingly, the discrepancy ratio between frontal and parietal pathways in measures of mean AD did not significantly differ between any of the groups, which contrasts with assessments of FA and RD indicating a greater reduction of WM integrity in posterior compared with anterior pathways in both groups with SBM compared with TD (Fig. 5). Despite no differences in ratios between groups, individuals with SBM and tectal beaking revealed a consistent overall increase in mean AD along both pathways when compared with TD controls and with individuals with SBM with a normal appearing tectum.

AD reflects the degree of diffusivity along the primary diffusion axis, and it has been previously related to variations of axonal integrity in animal models (Song et al., 2003). Thus, increased AD along both anterior and posterior tectocortical pathways unique to individuals with tectal beaking may implicate compromised axonal integrity secondary to developmental malformation of the tectum itself. The association between developmental structural malformation of the tectum and resulting decrements in DTI indicators of WM integrity along emanating tectocortical pathways is a novel finding, and may suggest a distinct correlate of change apart from the mechanical effects of hydrocephalus. Previous findings of supratentorial forebrain changes in individuals with SBM (such as "hypothalamic adhesion," abnormal placement of the anterior commissure, and gross abnormalities of the corpus callosum—distinguishable from classical commissural agenesis) have also supported a developmental basis for abnormalities in this population, arising distinct from changes commonly incurred by hydrocephalus (Miller et al., 2008). Ongoing studies implementing prenatal surgery to repair spinal meningomyelocele in SBM before birth may serve to clarify such issues. Although the precise mechanism relating tectal malformation to reductions in effective connectivity of this region is not well understood, tectal beaking is generally accepted to be indicative of greater severity of SBM and the Chiari II malformation, possibly suggesting an indirect link between the two (Barkovich and Raybaud, 2012).

Comparison of tectal volume

Contrary to the third hypothesis, regardless of qualitative evidence of tectal malformations, tectal volume was significantly decreased in individuals with SBM compared with TD controls. In other nonclinical literature, interest in the structure and function of the SC has been fueled by animal models recognizing the tectum as a critical component in nonreflexive attentional processing, with particular functional utility in attentional selection (Knudsen, 2011). Findings of reduced tectal volume in those with SBM, regardless of qualitative malformations in this region, is a novel contribution and provides evidence for potential neural correlates underlying attentional deficits observed in this population.

Conclusions

The current study helps elucidate the unique changes to tectocortical WM observed in SBM in the presence of hydrocephalus, with or without tectal malformation. Observed decrements in DTI metrics (FA and RD) indicative of WM integrity in SBM are most salient in posterior tectocortical pathways and may be more closely related to effects of congenital hydrocephalus. In addition, individuals with tectal beaking show increased AD along all tectocortical pathways, suggesting that some WM disruption may precede structural changes implicated by hydrocephalus. Furthermore, individuals with SBM, regardless of tectal malformations, show reductions in tectal volume compared with TD comparisons, which may also contribute to previously documented attentional processing deficits observed in this population.

Although the current study was limited by a 3 mm DTI slice thickness, which is not ideal for tractography success, output was observed to adequately reflect the pathways intended to be captured by the procedure. It would be of interest to replicate tectocortical pathway tractography in DTI scans with higher voxel resolution in future studies. Furthermore, constrained by the purely anatomical scope of the current study, inferences cannot be made directly linking structural findings to behavioral measures of attention. However, earlier research supports such a link, informing hypotheses tested in the current study predicting underlying neurostructural correlates of cognitive performance deficits observed in SBM. Future directions should incorporate behavioral attention data alongside DTI indices of WM structural integrity to further parse the unique contributions of the colliculus and emergent tectocortical pathways to cognitive function.

Acknowledgments

The authors would like to thank John Mosele for his assistance with data processing. This work is funded by NIH grant NICHD P01-HD35946 (to J.M.F.).

Author Disclosure Statement

No competing financial interests exist.

References

Aoyama Y, Kinoshita Y, Yokota A, Hamada T. 2006. Neuronal damage in hydrocephalus and its restoration by shunt insertion in experimental hydrocephalus: a study involving the neurofilament-immunostaining method. J Neurosurg 104(5 Suppl):332–339.

Au KS, Ashley-Koch A, Northrup H. 2010. Epidemiologic and genetic aspects of spina bifida and other neural tube defects. Dev Disabil Res Rev 16:6–15.

Barkovich AJ. 2005. *Pediatric Neuroimaging*. Philadelphia, PA: Lippincott Williams & Wilkins.

Barkovich AJ, Raybaud C. 2012. *Pediatric Neuroimaging*. Philadelphia: Wolters Kluwer Health/Lippincott Williams & Wilkins.

Behrens TE, Woolrich MW, Jenkinson M, Johansen-Berg H, Nunes RG, Clare S, Matthews PM, Brady JM, Smith SM. 2003. Characterization and propagation of uncertainty in diffusion-weighted MR imaging. Magn Reson Med 50:1077–1088.

Bowman RM, McLone DG. 2010. Neurosurgical management of spina bifida: research issues. Dev Disabil Res Rev 16:82–87.

Budde MD, Kim JH, Liang HF, Schmidt RE, Russell JH, Cross AH, Song SK. 2007. Toward accurate diagnosis of white matter pathology using diffusion tensor imaging. Magn Reson Med 57:688–695.

Caspers S, Eickhoff SB, Rick T, von Kapri A, Kuhlen T, Huang R, Shah NJ, Zilles K. 2011. Probabilistic fibre tract analysis of cytoarchitectonically defined human inferior parietal lobule areas reveals similarities to macaques. Neuroimage 58: 362–380.

Concha L, Gross DW, Wheatley BM, Beaulieu C. 2006. Diffusion tensor imaging of time-dependent axonal and myelin degradation after corpus callosotomy in epilepsy patients. Neuroimage 32:1090–1099.

Dale AM, Fischl B, Sereno MI. 1999. Cortical surface-based analysis. I. Segmentation and surface reconstruction. Neuroimage 9:179–194.

Dennis M, Edelstein K, Copeland K, Frederick J, Francis DJ, Hetherington R, Blaser SE, Kramer LA, Drake JM, Brandt ME, et al. 2005a. Covert orienting to exogenous and endogenous cues in children with spina bifida. Neuropsychologia 43:976–987.

Dennis M, Edelstein K, Copeland K, Frederick JA, Francis DJ, Hetherington R, Blaser SE, Kramer LA, Drake JM, Brandt ME, et al. 2005b. Space-based inhibition of return in children with spina bifida. Neuropsychology 19:456–465.

Entis JJ, Doerga P, Barrett LF, Dickerson BC. 2012. A reliable protocol for the manual segmentation of the human amygdala and its subregions using ultra-high resolution MRI. Neuroimage 60:1226–1235.

Eskandari R, McAllister JP, 2nd, Miller JM, Ding Y, Ham SD, Shearer DM, Way JS. 2004. Effects of hydrocephalus and ventriculoperitoneal shunt therapy on afferent and efferent connections in the feline sensorimotor cortex. J Neurosurg 101(2 Suppl):196–210.

Fischl B, Liu A, Dale AM. 2001. Automated manifold surgery: constructing geometrically accurate and topologically correct models of the human cerebral cortex. IEEE Trans Med Imaging 20:70–80.

Fischl B, Salat DH, Busa E, Albert M, Dieterich M, Haselgrove C, van der Kouwe A, Killiany R, Kennedy D, Klaveness S, et al. 2002. Whole brain segmentation: automated labeling of neuroanatomical structures in the human brain. Neuron 33:341–355.

Fischl B, Salat DH, van der Kouwe AJ, Makris N, Segonne F, Quinn BT, Dale AM. 2004a. Sequence-independent segmentation of magnetic resonance images. Neuroimage 23 Suppl 1:S69–S84.

Fischl B, Sereno MI, Dale AM. 1999. Cortical surface-based analysis. II: Inflation, flattening, and a surface-based coordinate system. Neuroimage 9:195–207.

Fischl B, van der Kouwe A, Destrieux C, Halgren E, Segonne F, Salat DH, Busa E, Seidman LJ, Goldstein J, Kennedy D, et al. 2004b. Automatically parcellating the human cerebral cortex. Cereb Cortex 14:11–22.

Fletcher JM, Brei TJ. 2010. Introduction: Spina bifida—a multidisciplinary perspective. Dev Disabil Res Rev 16:1–5.

Fletcher JM, Copeland K, Frederick JA, Blaser SE, Kramer LA, Northrup H, Hannay HJ, Brandt ME, Francis DJ, Villarreal G, et al. 2005. Spinal lesion level in spina bifida: a source of neural and cognitive heterogeneity. J Neurosurg 102(3 Suppl):268–279.

Gadsdon DR, Variend S, Emery JL. 1979. Myelination of the corpus callosum. II. The effect of relief of hydrocephalus upon the processes of myelination. Z Kinderchir Grenzgeb 28:314–321.

Gitelman DR, Parrish TB, Friston KJ, Mesulam MM. 2002. Functional anatomy of visual search: regional segregations within the frontal eye fields and effective connectivity of the superior colliculus. Neuroimage 15:970–982.

Hanlo PW, Gooskens RJ, van Schooneveld M, Tulleken CA, van der Knaap MS, Faber JA, Willemse J. 1997. The effect of intracranial pressure on myelination and the relationship with neurodevelopment in infantile hydrocephalus. Dev Med Child Neurol 39:286–291.

Herweh C, Akbar M, Wengenroth M, Blatow M, Mair-Walther J, Rehbein N, Nennig E, Schenk JP, Heiland S, Stippich C. 2009. DTI of commissural fibers in patients with Chiari II-malformation. Neuroimage 44:306–311.

Ignashchenkova A, Dicke PW, Haarmeier T, Thier P. 2004. Neuron-specific contribution of the superior colliculus to overt and covert shifts of attention. Nat Neurosci 7:56–64.

Juranek J, Dennis M, Cirino PT, El-Messidi L, Fletcher JM. 2010. The cerebellum in children with spina bifida and Chiari II malformation: quantitative volumetrics by region. Cerebellum 9:240–248.

Juranek J, Fletcher JM, Hasan KM, Breier JI, Cirino PT, Pazo-Alvarez P, Diaz JD, Ewing-Cobbs L, Dennis M, Papanicolaou AC. 2008. Neocortical reorganization in spina bifida. Neuroimage 40:1516–1522.

Juranek J, Salman MS. 2010. Anomalous development of brain structure and function in spina bifida myelomeningocele. Dev Disabil Res Rev 16:23–30.

Knudsen EI. 2011. Control from below: the role of a midbrain network in spatial attention. Eur J Neurosci 33:1961–1972.

Li L, Preuss TM, Rilling JK, Hopkins WD, Glasser MF, Kumar B, Nana R, Zhang X, Hu X. 2010. Chimpanzee (Pan troglodytes) precentral corticospinal system asymmetry and handedness: a diffusion magnetic resonance imaging study. PLoS One 5:e12886.

Lovejoy LP, Krauzlis RJ. 2010. Inactivation of primate superior colliculus impairs covert selection of signals for perceptual judgments. Nat Neurosci 13:261–266.

Maxwell SE, Delaney HD. 2004. *Designing Experiments and Analyzing Data*. New York, NY: Psychology Press.

Merker B. 2007. Consciousness without a cerebral cortex: a challenge for neuroscience and medicine. Behav Brain Sci 30:63–81; discussion 81–134.

Miller E, Widjaja E, Blaser S, Dennis M, Raybaud C. 2008. The old and the new: supratentorial MR findings in Chiari II malformation. Childs Nerv Syst 24:563–575.

Mysore SP, Knudsen EI. 2011. The role of a midbrain network in competitive stimulus selection. Curr Opin Neurobiol 21: 653–660.

Nummela SU, Krauzlis RJ. 2010. Inactivation of primate superior colliculus biases target choice for smooth pursuit, saccades, and button press responses. J Neurophysiol 104:1538–1548.

Olopade FE, Shokunbi MT, Siren AL. 2012. The relationship between ventricular dilatation, neuropathological and neurobehavioural changes in hydrocephalic rats. Fluids Barriers CNS 9:19.

Posner MI, Petersen SE. 1990. The attention system of the human brain. Annu Rev Neurosci 13:25–42.

Reigel D, Rotenstein D. 1994. Spina bifida. In: Cheek WR (ed.). *Pediatric Neurosurgery: Surgery of the Developing Nervous System*, 3rd edition. Philadelphia, PA: WB Saunders; pp. 51–76.

Sereno AB, Briand KA, Amador SC, Szapiel SV. 2006. Disruption of reflexive attention and eye movements in an individual with a collicular lesion. J Clin Exp Neuropsychol 28:145–166.

Simpson GV, Weber DL, Dale CL, Pantazis D, Bressler SL, Leahy RM, Luks TL. 2011. Dynamic activation of frontal, parietal, and sensory regions underlying anticipatory visual spatial attention. J Neurosci 31:13880–13889.

Smith SM. 2002. Fast robust automated brain extraction. Hum Brain Mapp 17:143–155.

Song SK, Sun SW, Ju WK, Lin SJ, Cross AH, Neufeld AH. 2003. Diffusion tensor imaging detects and differentiates axon and myelin degeneration in mouse optic nerve after retinal ischemia. Neuroimage 20:1714–1722.

Talamonti G, D'Aliberti G, Collice M. 2007. Myelomeningocele: long-term neurosurgical treatment and follow-up in 202 patients. J Neurosurg 107(5 Suppl):368–386.

Taylor HB, Landry SH, Barnes M, Swank P, Cohen LB, Fletcher J. 2010. Early information processing among infants with and without spina bifida. Infant Behav Dev 33:365–372.

Tubbs RS, Soleau S, Custis J, Wellons JC, Blount JP, Oakes WJ. 2004. Degree of tectal beaking correlates to the presence of nystagmus in children with Chiari II malformation. Childs Nerv Syst 20:459–461.

Vachha B, Adams RC, Rollins NK. 2006. Limbic tract anomalies in pediatric myelomeningocele and Chiari II malformation: anatomic correlations with memory and learning—initial investigation. Radiology 240:194–202.

Xue H, Srinivasan L, Jiang S, Rutherford M, Edwards AD, Rueckert D, Hajnal JV. 2007. Automatic cortical segmentation in the developing brain. Inf Process Med Imaging 20:257–269.

Yuan W, McKinstry RC, Shimony JS, Altaye M, Powell SK, Phillips JM, Limbrick DD, Jr., Holland SK, Jones BV, Rajagopal A, et al. 2013. Diffusion tensor imaging properties and neurobehavioral outcomes in children with hydrocephalus. AJNR Am J Neuroradiol 34:439–445.

Zijdenbos AP, Dawant BM, Margolin RA, Palmer AC. 1994. Morphometric analysis of white matter lesions in MR images: method and validation. IEEE Trans Med Imaging 13:716–724.

Address correspondence to:
Victoria J. Williams
Department of Psychology
University of Houston
2151 W. Holcombe Blvd.
222 Texas Medical Center Annex
Houston, TX 77024-5053

E-mail: tori85@gmail.com